

Hypoxia regulates Hippo signalling through the SIAH2 ubiquitin E3 ligase

Biao Ma¹, Yan Chen¹, Ling Chen¹, Hongcheng Cheng¹, Chenglong Mu¹, Jie Li¹, Ruize Gao¹, Changqian Zhou¹, Lei Cao¹, Jinhua Liu¹, Yushan Zhu^{1,3}, Quan Chen^{1,2,3} and Shian Wu^{1,3}

The Hippo signalling pathway plays important roles in animal development, physiology and tumorigenesis^{1–3}. Understanding how the activity of this pathway is regulated by the cellular microenvironment remains a major challenge. Here we elucidate a molecular mechanism by which hypoxia deactivates Hippo signalling. We demonstrate that the E3 ubiquitin ligase SIAH2 stimulates YAP by destabilizing LATS2, a critical component of the Hippo pathway, in response to hypoxia. Loss of SIAH2 suppresses tumorigenesis in a LATS2-dependent manner in a xenograft mouse model. We further show that YAP complexes with HIF1 α and is essential for HIF1 α stability and function in tumours *in vivo*. LATS2 is downregulated in human breast tumours and negatively correlates with SIAH2 expression levels, indicating that the SIAH2–LATS2 pathway may have a role in human cancer. Our data uncover oxygen availability as a microenvironment signal for the Hippo pathway and have implications for understanding the regulation of Hippo signalling in tumorigenesis.

The Hippo pathway is an evolutionarily conserved regulator that controls organ size and its dysregulation contributes to tumorigenesis^{1–3}. Core components of this pathway comprise a kinase cascade that includes MST (1 and 2) and LATS (1 and 2), which are homologous to Hippo and Warts in *Drosophila* respectively^{4–7}. MST1 and MST2 phosphorylate and activate LATS1 and LATS2 to phosphorylate YAP, the key downstream effector of Hippo signalling⁸, causing YAP cytoplasm retention and suppression of target genes involved in cell proliferation and survival^{9,10}. Although mutations of LATS1 or LATS2 are uncommon, dysfunction of either LATS1 or LATS2 can lead to a broad range of cancers^{11–14}, which underscores the importance of LATS regulation under physiological and pathophysiological conditions.

Maintenance of oxygen homeostasis is critical to metazoan development and physiology¹⁵ and oxygen deprivation is a common feature of solid tumours¹⁶. The E3 ligase SIAH2 is an essential

component of the hypoxia response pathway¹⁷ and is implicated in normal development and tumorigenesis¹⁸. To identify binding partners of SIAH2, we performed mass spectrometry analysis of the SIAH2-associated immunoprecipitated complex. As SIAH2 has a high rate of self-degradation and induces substrate degradation, we used Flag–SIAH2^{RM}, a dominant negative form^{17,19}, as a bait and uncovered LATS2 as a potential SIAH2-binding partner at high confidence^{20–22} (Supplementary Table 1).

Consistent with the mass spectrometry result, exogenously expressed Myc–LATS2 and Flag–SIAH2^{RM} were reciprocally co-immunoprecipitated (Fig. 1a,b). A series of truncated constructs were used to identify the precise binding region(s) that facilitated the interaction between LATS2 and SIAH2. The results revealed that both the amino- and carboxy-terminal halves of SIAH2 bound to LATS2 (Fig. 1c). Conversely, LATS2 (1–720) associated with SIAH2 strongly, whereas LATS2 (1–666) completely abolished the binding with SIAH2, suggesting that the region of amino acids 667–720 is required for LATS2 association with SIAH2 (Fig. 1d and Supplementary Fig. 1). Intriguingly, LATS2 (667–1088) had much less binding activity (Fig. 1d and Supplementary Fig. 1), despite it harbouring the critical region of amino acids 667–720, suggesting that another N-terminal region may facilitate LATS2–SIAH2 binding. Consistently, LATS2 (Δ 403–480), an internal deletion of LATS2, decreased its ability to associate with SIAH2 (Fig. 1d and Supplementary Fig. 1). Taken together, LATS2 contains at least two critical regions for its association with SIAH2: amino acids 403–480 and amino acids 667–720 (Fig. 1e). This interaction between SIAH2 and LATS2 was further demonstrated to be direct by *in vitro* pulldown assays (Fig. 1f).

As SIAH2 functions as an E3 ubiquitin ligase²³, we first examined whether LATS2 stability is regulated by SIAH2 and found SIAH2, but not SIAH2^{RM}, reduced LATS2 protein levels in a dosage-dependent manner (Supplementary Fig. 2a,b). In contrast, the protein levels of LATS2 (1–666), which is unable to bind SIAH2, were not affected

¹State Key Laboratory of Medicinal Chemical Biology, Tianjin Key Laboratory of Protein Sciences, College of Life Sciences, Nankai University, Tianjin 300071, China.

²State Key Laboratory of Biomembrane and Membrane Biotechnology, Institute of Zoology, Chinese Academy of Sciences, Beijing 100101, China.

³Correspondence should be addressed to Y.Z., Q.C. or S.W. (e-mail: zhuy@nankai.edu.cn or chenq@ioz.ac.cn or wusa@nankai.edu.cn)

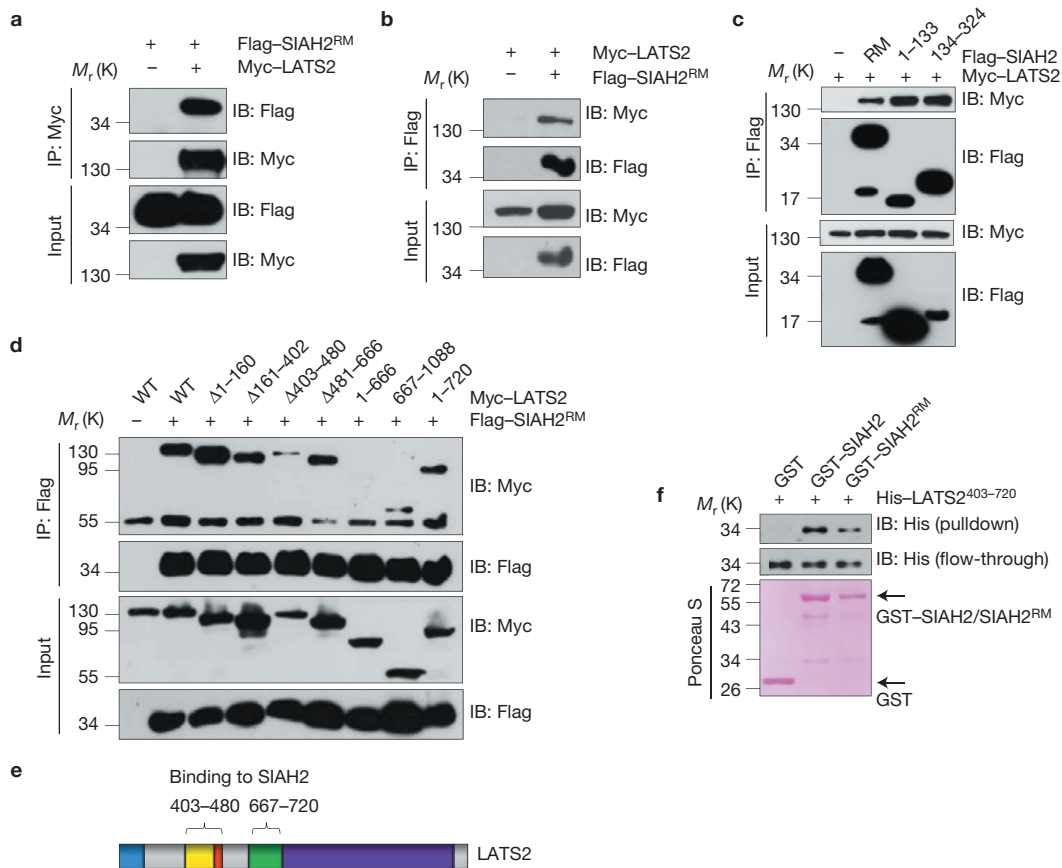


Figure 1 SIAH2 interacts with LATS2 *in vivo* and *in vitro*. (**a,b**) Co-immunoprecipitation of exogenously expressed Flag-SIAH2^{RM} with Myc-LATS2 (**a**) and vice versa (**b**) in HEK293T cells. (**c**) Co-immunoprecipitation of exogenously expressed Myc-LATS2 with the N- or C-terminal half of Flag-SIAH2. (**d,e**) Dissection of the critical regions of LATS2 through

co-immunoprecipitation in HEK293T cells (**d**), and a schematic drawing of the two critical binding regions of LATS2 (**e**) for SIAH2 binding (domain details described in Supplementary Fig. 1). (**f**) Direct interaction between bacterially expressed His-LATS2 (403–720) and GST-SIAH2 or GST-SIAH2^{RM} *in vitro*. Uncropped images of blots are shown in Supplementary Fig. 5.

by SIAH2 (Supplementary Fig. 1), suggesting that SIAH2–LATS2 association is important for SIAH2-induced LATS2 downregulation. Furthermore, a proteasomal inhibitor MG132 completely reversed LATS2 destabilization, whereas a lysosomal inhibitor bafilomycin A1 (BA1) had no such effect (Supplementary Fig. 2c,d), suggesting that SIAH2 initiated LATS2 reduction through the proteasome pathway. Consistently, stable expression of SIAH2 or SIAH2^{RM} reduced or increased the endogenous LATS2 levels respectively (Fig. 2a). Conversely, SIAH2 knockdown caused accumulation of endogenous LATS2 (Fig. 2b), demonstrating that SIAH2 is a negative regulator of LATS2 *in vivo*. Cycloheximide chase assays further showed that the half-life of either endogenous (Fig. 2c–f) or exogenous (Supplementary Fig. 2e,f) LATS2 was significantly shortened in the presence of SIAH2 but not SIAH2^{RM} or SIAH2 knockdown.

Next, we investigated whether degradation of LATS2 was mediated through ubiquitylation and found that the dominant-negative SIAH2^{RM} or SIAH2 knockdown decreased the ubiquitylation of co-transfected (Fig. 2g) or endogenous LATS2 (Fig. 2h). Furthermore, *in vitro* ubiquitylation assays showed that LATS2 was ubiquitylated by SIAH2 but not SIAH2^{RM} (Fig. 2i). To identify the potential ubiquitylation site(s), we aligned the C-terminal LATS2 (667–1088) of 28 vertebrate species with *Drosophila* Warts and identified 9

conserved lysine residues (Fig. 3j and Supplementary Table 2). By mutating each lysine to arginine, we found that mutation of Lys 670 or Lys 672 renders LATS2 less responsive to SIAH2-mediated downregulation, and a double mutation of Lys 670 and Lys 672 renders LATS2 nearly completely unresponsive to SIAH2-mediated degradation and ubiquitylation (Fig. 3k,l). Thus, multiple lysine residues in LATS2 might respond to SIAH2-mediated ubiquitylation, and among of them, Lys 670 and Lys 672 are two key sites.

YAP-S127 phosphorylation is a direct readout of LATS kinase activity⁹. Concomitant with SIAH2-induced downregulation of LATS2, YAP-S127 phosphorylation was significantly reduced (Fig. 2a,b) and YAP nuclear translocation was enhanced (Fig. 2m). Conversely, SIAH2^{RM} overexpression or SIAH2 knockdown resulted in LATS2 accumulation, increased YAP-S127 phosphorylation (Fig. 2a,b) and decreased YAP nuclear localization (Fig. 2m). The phospho-defective mutant YAP-S127A, which is constitutively located in the nucleus, was not affected by SIAH2^{RM} (Fig. 2m), indicating that SIAH2-induced YAP nuclear translocation depends on the phosphorylation status of YAP-S127. Taken together, these results uncover that SIAH2 antagonizes Hippo signalling and activates YAP by promoting the ubiquitylation and degradation of LATS2.

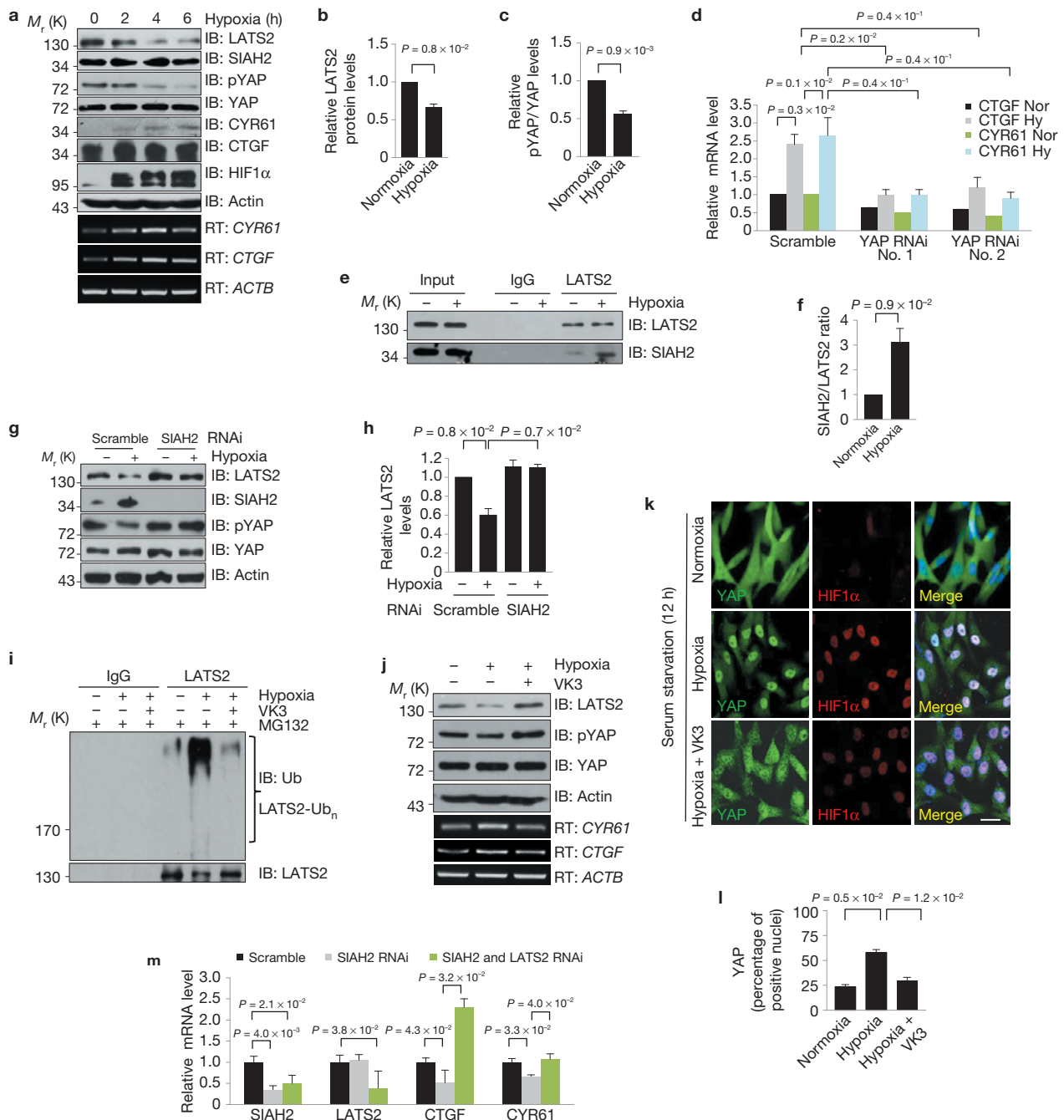


Figure 3 Hypoxia deactivates Hippo signalling through SIAH2-dependent degradation of LATS2. **(a)** MDA-MB-231 cells cultured under hypoxia were analysed by immunoblotting using the indicated antibodies or by PCR with reverse transcription (RT-PCR) for the indicated genes at the indicated time points. **(b,c)** Quantitative analysis of LATS2 **(b)** and phosphorylation of YAP **(c)** in MDA-MB-231 cells cultured under hypoxia for 6 h. **(d)** Scramble and YAP-knockdown MDA-MB-231 cells were cultured under normoxia or hypoxia for 6 h. The indicated genes were analysed by real-time PCR (RT-qPCR). **(e,f)** MDA-MB-231 cells were treated with 10 μ M MG132 and incubated under normoxia or hypoxia for 4 h. Endogenous interaction between LATS2 and SIAH2 was analysed by immunoprecipitation **(e)**, and binding intensity was quantified **(f)**. **(g,h)** Scramble and SIAH2-knockdown MDA-MB-231 cells were cultured under normoxia or hypoxia for 4 h, and then collected for western blotting using the indicated antibodies **(g)** and quantification of LATS2 protein levels (normalized to actin) **(h)**. **(i)** MDA-MB-231 cells were pretreated with or without vitamin K3 (50 μ M) for 1 h, followed by incubation

under normoxia or hypoxia in the presence of 10 μ M MG132 for another 6 h. Cell lysates were immunoprecipitated with LATS2 antibodies and then detected by western blotting with the indicated antibodies. **(j)** MDA-MB-231 cells were pretreated with or without vitamin K3 (50 μ M) for 1 h, followed by incubation under normoxia or hypoxia for another 6 h. Cells were analysed by immunoblotting using the indicated antibodies or RT-PCR analysis for the indicated genes. **(k)** MDA-MB-231 cells were serum starved for 12 h, and then pretreated with vitamin K3 (50 μ M) for 1 h before incubation under normoxia or hypoxia for another 6 h. Scale bars, 25 μ m. **(l)** Quantitative analysis of YAP nuclear translocation. **(m)** SIAH2-knockdown or SIAH2 and LATS2 double-knockdown MDA-MB-231 cells were cultured under hypoxic conditions. Total RNA was extracted and subjected to RT-qPCR analysis for the indicated genes. All data are the mean of $n = 3$ independent experiments. All error bars indicate s.d. Significance is determined by two-tailed, unpaired Student's *t*-test. Uncropped images of blots are shown in Supplementary Fig. 5.

The human genome encodes two SIAH proteins, SIAH1 and SIAH2 (ref. 24). In contrast to SIAH2, SIAH1 did not co-immunoprecipitate with LATS2 (Supplementary Fig. 3a) or promote LATS2 degradation (Supplementary Fig. 3b). LATS1 and LATS2 are the two human homologues of *Drosophila* Warts^{25,26}. We expected that SIAH2 could similarly regulate LATS1 and LATS2. Indeed, SIAH2 interacted with LATS1 and induced its degradation (Supplementary Fig. 3c,d), suggesting that SIAH2 may regulate both LATS1 and LATS2 stability through similar mechanisms. In addition, we did not detect any interaction between SIAH1 and LATS1 (Supplementary Fig. 3e). Thus, LATS1 and LATS2 seem to be specifically regulated by SIAH2 but not SIAH1.

As SIAH2 is a well-established regulator of hypoxia response^{17,23,27}, we examined the effect of hypoxia on LATS2 stability and Hippo signalling. In MDA-MB-231 cells, LATS2 abundance and YAP-S127 phosphorylation were significantly reduced under hypoxia (Fig. 3a–c) and YAP nuclear localization was also enhanced (Fig. 3k,l). These results suggest that hypoxia induced LATS2 degradation and subsequently de-repressed YAP activity. Consistent with this notion, both the protein and messenger RNA levels of well-established Hippo target genes such as *CYR61* and *CTGF* were increased (Fig. 3a,d). Conversely, knockdown of YAP attenuated the transcriptional upregulation of *CYR61* and *CTGF* induced by hypoxia (Fig. 3d), indicating that hypoxia-induced Hippo target expression is YAP-dependent. Importantly, the interaction between LATS2 and SIAH2 was significantly enhanced under hypoxic conditions (Fig. 3e,f), supporting the finding that SIAH2 is responsible for LATS2 turnover and Hippo signalling transduction under hypoxia. Indeed, SIAH2 inhibition by vitamin K3 (an inhibitor of SIAH2; refs 27,28) or SIAH2 knockdown attenuated the effects of hypoxia on LATS2 ubiquitylation (Fig. 3i) and degradation (Fig. 3g,h,j), YAP dephosphorylation (Fig. 3g,j), nuclear translocation (Fig. 3k,l) and expression of the Hippo targets *CTGF* and *CYR61* (Fig. 3j,m). It is noteworthy that simultaneous knockdown of LATS2 and SIAH2 protected hypoxia-induced Hippo target expression from SIAH2 depletion (Fig. 4m), suggesting that LATS2 is a downstream effector of SIAH2 and hypoxia-regulated Hippo signalling depends on SIAH2-induced LATS2 degradation.

To investigate the biological relevance of SIAH2-induced degradation of LATS2, we first assessed the properties of SIAH2 in regulation of cell proliferation and cell death. Stably expressed SIAH2 increased cell proliferation and cell viability; however, SIAH2^{RM} had no such effects (Fig. 4a,b). Conversely, SIAH2 knockdown markedly decreased colony-formation rate and increased cell apoptosis under hypoxia, which were attenuated by concomitant knockdown of LATS2 (Fig. 4c,d). Next, we subcutaneously implanted cells with SIAH2 single knockdown or SIAH2 and LATS2 double knockdown into nude mice and monitored tumour growth. Mice bearing SIAH2-silenced cells showed a 5.8-fold and 4.6-fold decrease in tumour weight and volume compared with the scramble group respectively (Fig. 4e–g). Notably, simultaneous knockdown of LATS2 expression fully reversed the tumour-inhibiting effect of SIAH2 knockdown (Fig. 4e–g). Immunohistochemical analysis of the implanted tumours revealed increased intensity of LATS2 and pYAP and reduced Ki67-positive proliferative cells in SIAH2-knockdown tumours (Fig. 4h), whereas concomitant knockdown of LATS2 attenuated such effects (Fig. 4h).

Therefore, loss of SIAH2 inhibits tumorigenesis through stabilizing LATS2 and upregulating pYAP.

Tumour cells are normally situated in hypoxia microenvironments¹⁶ and LATS2 is a tumour suppressor whose loss-of-function leads to tumour development in many mammalian tissues^{11–14}. To determine the correlation between LATS2 and SIAH2 in patients, we examined their expression levels in breast cancer tissue microarrays. Notably, low expression of LATS2 was observed in 68% (138 of 203) of breast tumours and 25.7% (18 of 70) of normal breast tissues, indicating a statistically significant correlation between breast tumorigenesis and LATS2 downregulation (Supplementary Table 3). However, high expression of SIAH2 was observed in 48.5% (99 of 204) of breast tumours compared with 10.4% (8 of 77) of normal breast tissues, suggesting another significant correlation between SIAH2 upregulation and tumorigenesis (Supplementary Table 3). Collectively, these results suggest a possible link between low LATS2 and high SIAH2 expression in human breast tumours. Indeed, using serial sections and statistical analysis tools we found that the protein levels of SIAH2 and LATS2 are significantly inversely correlated in breast tumour tissues (Fig. 4i,j and Supplementary Table 3).

TAZ, a paralogue of YAP in mammals, was recently reported to facilitate HIF1 α activity^{29,30}, but the molecular mechanism was not clear. We were interested to investigate the effect of YAP on hypoxia response and found that YAP knockdown greatly decreased hypoxia-induced HIF1 α accumulation (Fig. 5a) without significant changes in HIF1 α mRNA levels (Supplementary Fig. 4a). Intriguingly, MG132 fully rescued this phenotype (Supplementary Fig. 4b), indicating that YAP knockdown promotes proteasome-mediated degradation of HIF1 α . To examine the consequences of this phenomenon *in vivo*, we subcutaneously implanted YAP knockdown cells into nude mice and monitored tumour growth. Mice bearing YAP-silenced cells showed decreased tumour growth as evidenced by a 2.8- and 2.4-fold reduction in tumour volume and tumour weight respectively (Fig. 5b–d). Moreover, immunohistochemical staining of the xenograft tumour tissues showed that loss of YAP impaired HIF1 α accumulation (Fig. 5e), decreased microvessel density (Fig. 5e,f) and reduced Ki67-positive cells (Fig. 5e), indicating that YAP may facilitate tumour growth and angiogenesis through stabilizing HIF1 α *in vivo*. Consistent with these results, knockdown of YAP greatly reduced HIF1 α target VEGF expression (Fig. 5g). Furthermore, LATS2 overexpression decreased hypoxia-induced activation of a HRE-luciferase reporter, whereas concomitant expression of YAP-S127A could rescue this effect (Fig. 5h), indicating that YAP de-repression from LATS2 is required for maximum HIF1 α activity. Indeed, LATS2 overexpression also inhibited HIF1 α accumulation and the kinase-dead mutant of LATS2 failed (Fig. 5i), indicating that LATS2 kinase activity is required for HIF1 α regulation and this may explain why LATS2 impaired HIF1 α activity, whereas overexpression of YAP-S127A restored it.

To further assess the effect of YAP on HIF1 α stability, we re-expressed YAP in YAP-knockdown cells and found that wild-type YAP or the phospho-defective mutant YAP-S127A fully restored HIF1 α accumulation under hypoxia but the phospho-mimetic mutant YAP-S127D did not (Fig. 5i,j), indicating that the phosphorylation status of YAP is crucial for HIF1 α stabilization. To our surprise, YAP is not only required for HIF1 α accumulation under hypoxia, but also sufficient to keep HIF1 α constant under normoxia

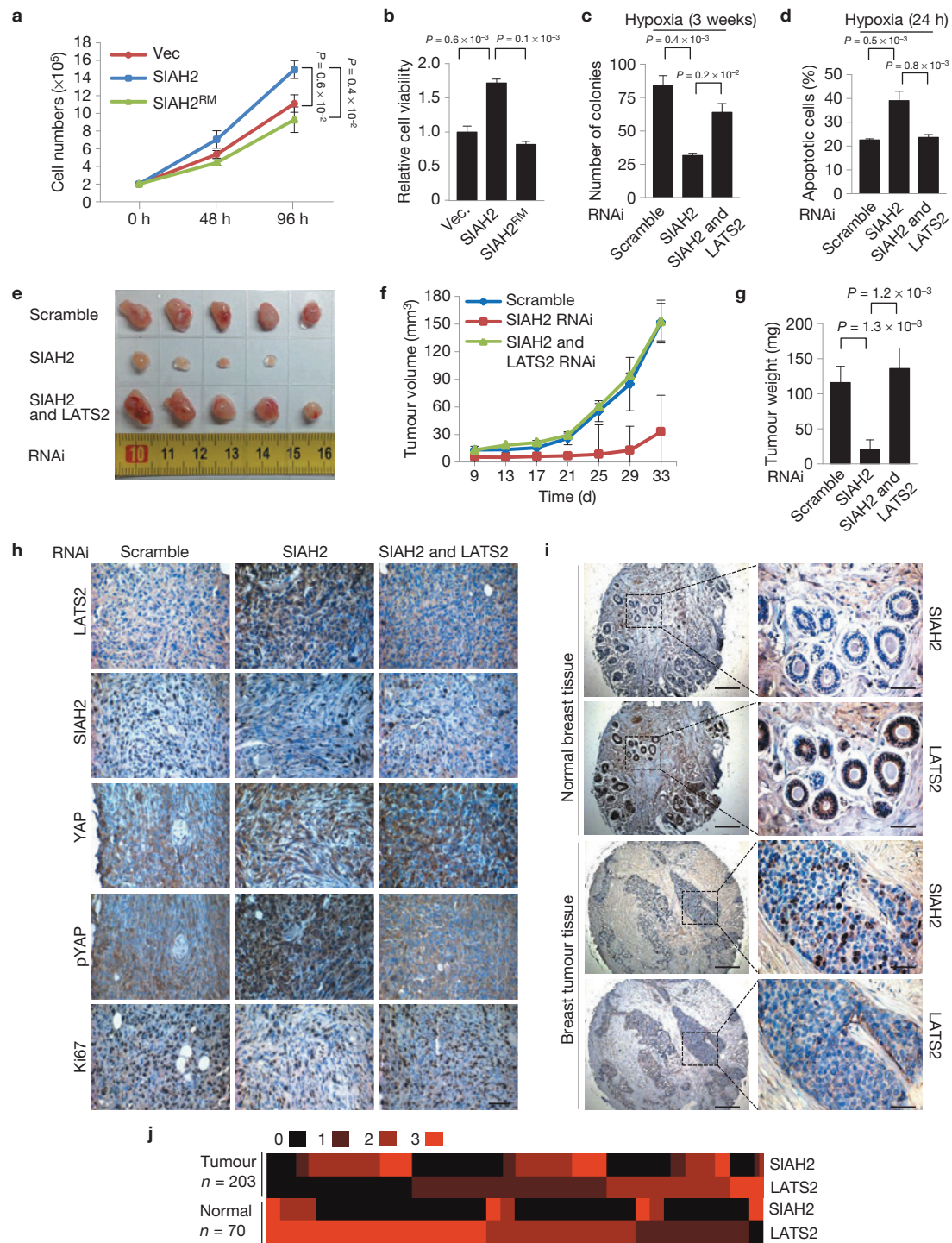


Figure 4 SIAH2 promotes tumour growth through downregulation of LATS2. (a,b) Cell proliferation rate (a) and relative cell viability (b) of MDA-MB-231 cells stably transfected with SIAH2 or SIAH2^{RM} cultured under normoxic conditions. (c) Colony-formation rate of SIAH2-knockdown and SIAH2 and LATS2 double-knockdown MDA-MB-231 cells cultured under hypoxic conditions for 3 weeks. (d) Apoptotic rate of SIAH2-knockdown and SIAH2 and LATS2 double-knockdown MDA-MB-231 cells cultured under hypoxic conditions for 24 h. (e–g) Tumour images (e), tumour growth curves (f) and tumour weight (g) of mice with subcutaneous injection of SIAH2-knockdown or SIAH2 and LATS2 double-knockdown MDA-MB-231 cells. (h) Immunohistochemical analysis of SIAH2-knockdown and SIAH2 and LATS2 double-knockdown xenograft tumour tissues with the indicated

antibodies. (Brown colour indicates a positive immune reaction; scale bars, 50 μ m.) (i) Immunohistochemical staining of LATS2 and SIAH2 in representative normal breast tissues and breast tumour tissues on the tissue microarrays. (Brown colour indicates positive immune reaction; scale bars, (left) 200 μ m; (right) 50 μ m.) (j) Heat map of the expression of LATS2 and SIAH2 in human normal breast tissues and breast tumour tissues. $n = 203$ breast tumours and $n = 70$ normal breast tissue samples. Data in a,c,d are the mean of $n = 3$ independent experiments and in b are the mean of $n = 4$ independent experiments. $n = 5$ mice per group in e–g. All error bars indicate s.d. Significance is determined by two-tailed, unpaired Student's *t*-test. The statistical data for i and j can be found in Supplementary Table 3. The source data for a–d can be found in Supplementary Table 4.

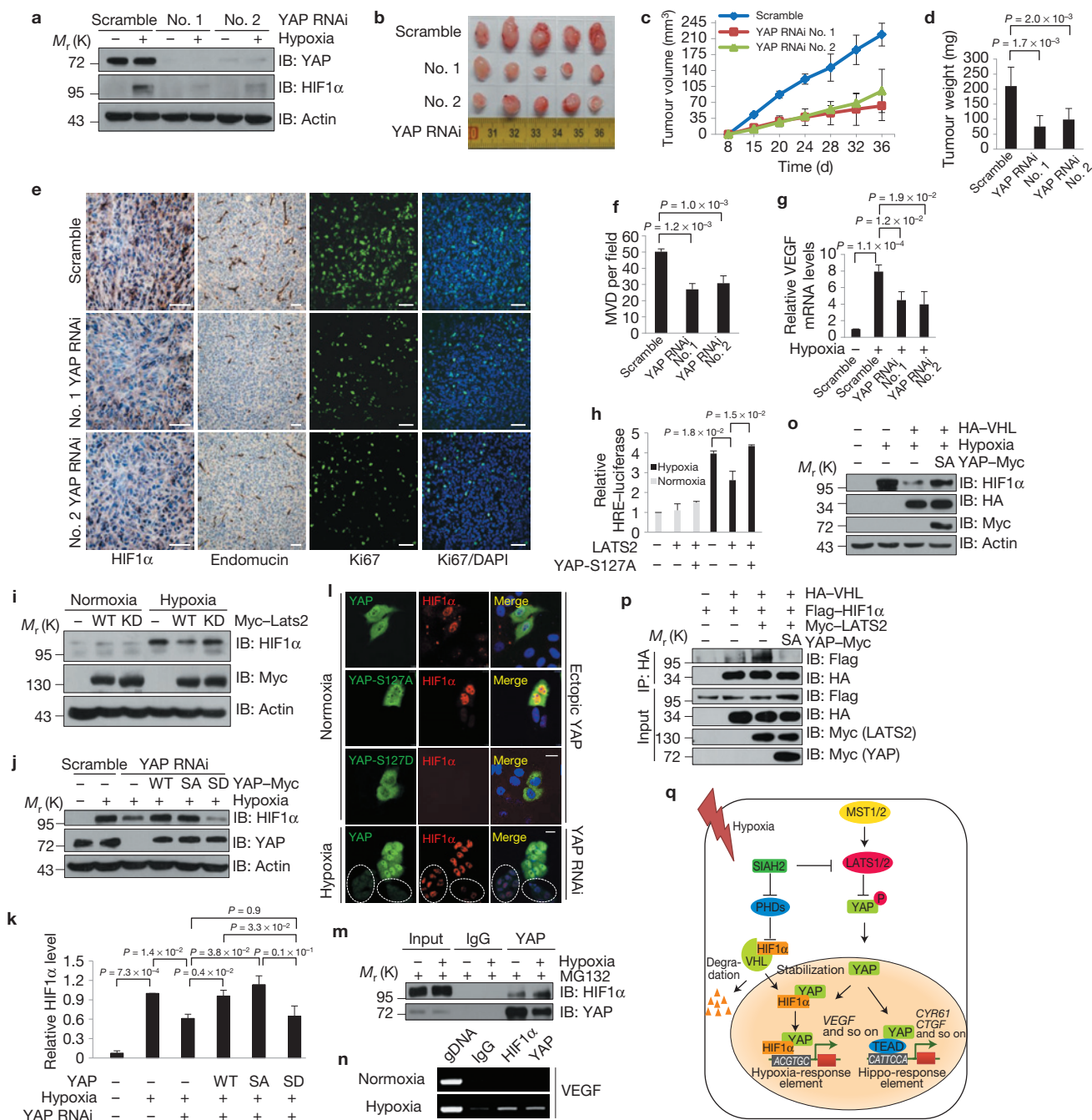


Figure 5 YAP interacts with HIF1 α and promotes its stabilization under hypoxia. (a) Immunoblotting of YAP and HIF1 α in scramble and YAP-knockdown MDA-MB-231 cells cultured under normoxia or hypoxia. (b–d) Tumour images (b), tumour growth curves (c) and tumour weight (d) of mice with subcutaneous injection of MDA-MB-231 cells with or without knock-down of YAP. (e) Immunohistochemical analysis of xenograft tumour tissues with the indicated antibodies. Scale bars, 50 μ m. (f) Quantitative analysis of microvessel density (MVD) in xenograft tumour sections. (g) RT-qPCR analysis for VEGF mRNA expression of scramble and YAP-knockdown MDA-MB-231 cells cultured under normoxia or hypoxia. (h) HIF1 α activity was determined by HRE-luciferase assay under normoxia or hypoxia in the presence of LATS2 or together with YAP-S127A. (i) Cells were transduced with LATS2 or LATS2 kinase-dead mutant (KD). Twenty-four hours later, cells were incubated under normoxia or hypoxia for 6 h. (j) YAP-knockdown cells were transfected with the indicated plasmids; wild type (WT), YAP-S127A (SA), YAP-S127D (SD). Twenty-four hours later, cells were incubated under normoxia or hypoxia for 6 h. (k) Quantitative analysis of HIF1 α

protein levels. (l) YAP-transfected or YAP-mutant-transfected HeLa cells and YAP-knockdown HeLa cells were incubated under normoxia or hypoxia for 6 h. Scale bars, 20 μ m. (m) Co-immunoprecipitation of endogenous YAP and HIF1 α in MDA-MB-231 cells under normoxia and hypoxia in the presence of 10 μ M MG132 (n) MDA-MB-231 cells were cultured under normoxia or hypoxia for 6 h. Lysates were then subjected to chromatin immunoprecipitation assay, and the products of the assay were amplified by PCR reaction. (o) Cells were transfected with HA-VHL alone or together with YAP-S127A (SA). Twenty-four hours later, cells were incubated under normoxia or hypoxia for 6 h. (p) Co-immunoprecipitation of exogenously expressed HIF1 α with VHL in the presence of LATS2 alone or together with YAP-S127A (SA) in HEK293 cells. (q) A proposed model of crosstalk between Hippo signalling and hypoxia response. Data in f–h and k are the mean of $n=3$ independent experiments. $n=5$ mice per group in b–d. All error bars indicate s.d. Significance is determined by two-tailed, unpaired Student's t -test. Uncropped images of blots are shown in Supplementary Fig. 5.

(Fig. 5l). Taken together, our results suggest that hypoxia-mediated LATS2 degradation and subsequently YAP dephosphorylation is important for HIF1 α stabilization. Given hypoxia-triggered YAP nuclear translocation (Fig. 3k), we reason that YAP may complex with HIF1 α in the nucleus. Indeed, YAP and HIF1 α were co-immunoprecipitated and their interaction was enhanced under hypoxic conditions (Fig. 5m). Chromatin immunoprecipitation assay further demonstrated that YAP complexed with HIF1 α at the HRE site within the VEGF promoter region in response to hypoxia (Fig. 5n).

Hydroxylation of HIF1 α is prerequisite for its degradation by binding to the E3 ubiquitin ligase VHL (refs 31,32). We wondered whether YAP-mediated HIF1 α stabilization depends on its hydroxylation changes and found that loss of YAP did not affect HIF1 α hydroxylation (Supplementary Fig. 4c). On the other hand, ectopic expression of YAP-S127A inhibited VHL-mediated HIF1 α degradation (Fig. 5o). Furthermore, overexpression of LATS2 enhanced HIF1 α -VHL interaction and concomitant expression of YAP-S127A attenuated this effect (Fig. 5p), indicating that the LATS2-YAP axis regulates HIF1 α -VHL complex assembly and HIF1 α stability.

Intrinsic and extrinsic factors must act coordinately to specify proper cell fate and tissue size. The Hippo tumour suppression pathway is evolutionarily conserved to limit tissue growth^{3,33-36}, but how extrinsic cues regulate Hippo signalling remains a major challenge. Our study demonstrates that oxygen availability acts as an extrinsic cue that regulates Hippo signalling through SIAH2-mediated turnover of LATS2, and the Hippo signalling effector YAP regulates the stability and function of HIF1 α (Fig. 5q). Hypoxia in the tumour microenvironment can arise as a consequence of tumour development and could also become limiting for tumour growth^{15,37}, raising the question of the significance of hypoxia-induced YAP activity in tumorigenesis. It is possible that, during early tumour development, oxygen levels are sufficient and SIAH2 levels are kept low, resulting in relatively high LATS2 levels that can suppress YAP activity. However, the development of a hypoxic microenvironment during tumour growth leads to SIAH2 accumulation and subsequent LATS2 degradation, which results in YAP activation to ensure the continuous survival and growth of tumour cells under hypoxia. Moreover, we show that YAP is important for HIF1 α stability and activity during hypoxia (Fig. 5a,g), and that YAP-silenced xenograft tumours exhibit impaired HIF1 α expression and microvessel formation (Fig. 5e,f), indicating that YAP may have an important role in the hypoxia response in addition to its well-known growth-promoting function. Thus, hypoxia-induced YAP and HIF1 α activation may together play a pro-survival role for hypoxic tumours. Further understanding of the biological significance of how YAP and HIF1 α are coordinated in response to hypoxia could provide insight into therapeutic strategies against diseases that are associated with aberrant activities of these pathways. □

METHODS

Methods and any associated references are available in the [online version of the paper](#).

Note: Supplementary Information is available in the [online version of the paper](#)

ACKNOWLEDGEMENTS

We thank H. Deng from Tsinghua University for Mass spectrometry analysis, Y. (YZ) Luo from Tsinghua University for providing the HRE-luciferase reporter plasmid and Y. (YG) Chen from Tsinghua University for providing the HA-VHL plasmid. We are deeply grateful to D. (DJ) Pan from Johns Hopkins University for his suggestions during the manuscript revision. This work was supported by the National Basic Research Program of China (2010CB912204, 2011CB9109903, 2011CB943903 and 2013CB531200) and the National Natural Sciences Foundation of China (31471319, 81130045 and 31171411).

AUTHOR CONTRIBUTIONS

B.M. conceived and designed the experiments with Y.Z., Q.C. and S.W. B.M. performed most of the experiments and data analysis in the laboratories of Q.C. and Y.Z. B.M., C.M. and R.G. performed xenograft implantation experiments. B.M. and C.M. performed studies on tissue microarrays of human patient samples. L. Chen, H.C. and J. Li contributed to cellular experiments and plasmid construction and protein purification. Y.C., L. Cao, C.Z. and J. Liu provided technical support. B.M. and S.W. wrote the manuscript with the help of all authors. Q.C. initiated, and supervised the project together with Y.Z. and S.W.

COMPETING FINANCIAL INTERESTS

The authors declare no competing financial interests.

Published online at www.nature.com/doi/10.1038/ncb3073

Reprints and permissions information is available online at www.nature.com/reprints

- Pan, D. The hippo signaling pathway in development and cancer. *Dev. Cell* **19**, 491–505 (2010).
- Harvey, K. F., Zhang, X. & Thomas, D. M. The Hippo pathway and human cancer. *Nat. Rev. Cancer* **13**, 246–257 (2013).
- Zhao, B., Tumaneng, K. & Guan, K. L. The Hippo pathway in organ size control, tissue regeneration and stem cell self-renewal. *Nat. Cell Biol.* **13**, 877–883 (2011).
- Wu, S., Huang, J., Dong, J. & Pan, D. hippo encodes a Ste-20 family protein kinase that restricts cell proliferation and promotes apoptosis in conjunction with salvador and warts. *Cell* **114**, 445–456 (2003).
- Harvey, K. F., Pflieger, C. M. & Hariharan, I. K. The *Drosophila* Mst ortholog, hippo, restricts growth and cell proliferation and promotes apoptosis. *Cell* **114**, 457–467 (2003).
- Pantalacci, S., Tapon, N. & Leopold, P. The Salvador partner Hippo promotes apoptosis and cell-cycle exit in *Drosophila*. *Nat. Cell Biol.* **5**, 921–927 (2003).
- Udan, R. S., Kango-Singh, M., Nolo, R., Tao, C. & Halder, G. Hippo promotes proliferation arrest and apoptosis in the Salvador/Warts pathway. *Nat. Cell Biol.* **5**, 914–920 (2003).
- Huang, J., Wu, S., Barrera, J., Matthews, K. & Pan, D. The Hippo signaling pathway coordinately regulates cell proliferation and apoptosis by inactivating Yorkie, the *Drosophila* homolog of YAP. *Cell* **122**, 421–434 (2005).
- Dong, J. *et al.* Elucidation of a universal size-control mechanism in *Drosophila* and mammals. *Cell* **130**, 1120–1133 (2007).
- Zhao, B. *et al.* Inactivation of YAP oncoprotein by the Hippo pathway is involved in cell contact inhibition and tissue growth control. *Genes Dev.* **21**, 2747–2761 (2007).
- Hisaoaka, M., Tanaka, A. & Hashimoto, H. Molecular alterations of h-warts/LATS1 tumour suppressor in human soft tissue sarcoma. *Lab. Invest.* **82**, 1427–1435 (2002).
- Jimenez-Velasco, A. *et al.* Downregulation of the large tumor suppressor 2 (LATS2/KPM) gene is associated with poor prognosis in acute lymphoblastic leukemia. *Leukemia* **19**, 2347–2350 (2005).
- Ishizaki, K. *et al.* Frequent polymorphic changes but rare tumor specific mutations of the LATS2 gene on 13q11-12 in esophageal squamous cell carcinoma. *Int. J. Oncol.* **21**, 1053–1057 (2002).
- Powzaniuk, M. *et al.* The LATS2/KPM tumor suppressor is a negative regulator of the androgen receptor. *Mol. Endocrinol.* **18**, 2011–2023 (2004).
- Semenza, G. L. Hypoxia-inducible factors in physiology and medicine. *Cell* **148**, 399–408 (2012).
- Brown, J. M. & Wilson, W. R. Exploiting tumour hypoxia in cancer treatment. *Nat. Rev. Cancer* **4**, 437–447 (2004).
- Nakayama, K. *et al.* Siah2 regulates stability of prolyl-hydroxylases, controls HIF1 α abundance, and modulates physiological responses to hypoxia. *Cell* **117**, 941–952 (2004).
- Nakayama, K., Qi, J. & Ronai, Z. The ubiquitin ligase Siah2 and the hypoxia response. *Mol. Cancer Res.* **7**, 443–451 (2009).
- Qi, J. *et al.* Siah2-dependent concerted activity of HIF and FoxA2 regulates formation of neuroendocrine phenotype and neuroendocrine prostate tumors. *Cancer Cell* **18**, 23–38 (2010).
- Calzado, M. A., de la Vega, L., Moller, A., Bowtell, D. D. & Schmitz, M. L. An inducible autoregulatory loop between HIPK2 and Siah2 at the apex of the hypoxic response. *Nat. Cell Biol.* **11**, 85–91 (2009).
- Habelhah, H. *et al.* Regulation of 2-oxoglutarate (alpha-ketoglutarate) dehydrogenase stability by the RING finger ubiquitin ligase Siah. *J. Biol. Chem.* **279**, 53782–53788 (2004).

22. Christian, P. A., Fiandalo, M. V. & Schwarze, S. R. Possible role of death receptor-mediated apoptosis by the E3 ubiquitin ligases Siah2 and POSH. *Mol. Cancer* **10**, 57 (2011).
23. Wong, C. S. & Moller, A. Siah: a promising anticancer target. *Cancer Res.* **73**, 2400–2406 (2013).
24. Hu, G. *et al.* Characterization of human homologs of the *Drosophila* seven in absentia (sina) gene. *Genomics* **46**, 103–111 (1997).
25. Tao, W. *et al.* Human homologue of the *Drosophila melanogaster* lats tumour suppressor modulates CDC2 activity. *Nat. Genet.* **21**, 177–181 (1999).
26. Yabuta, N. *et al.* Structure, expression, and chromosome mapping of LATS2, a mammalian homologue of the *Drosophila* tumor suppressor gene lats/warts. *Genomics* **63**, 263–270 (2000).
27. Sun, R. C. & Denko, N. C. Hypoxic regulation of glutamine metabolism through HIF1 and SIAH2 supports lipid synthesis that is necessary for tumor growth. *Cell Metab.* **19**, 285–292 (2014).
28. Shah, M. *et al.* Inhibition of Siah2 ubiquitin ligase by vitamin K3 (menadione) attenuates hypoxia and MAPK signaling and blocks melanoma tumorigenesis. *Pigment Cell Melanoma Res.* **22**, 799–808 (2009).
29. Bendinelli, P. *et al.* Hypoxia inducible factor-1 is activated by transcriptional co-activator with PDZ-binding motif (TAZ) versus WWdomain-containing oxidoreductase (WWOX) in hypoxic microenvironment of bone metastasis from breast cancer. *Eur. J. Cancer* **49**, 2608–2618 (2013).
30. Matteucci, E. *et al.* Bone metastatic process of breast cancer involves methylation state affecting E-cadherin expression through TAZ and WWOX nuclear effectors. *Eur. J. Cancer* **49**, 231–244 (2013).
31. Kaelin, W. G. Jr. & Ratcliffe, P. J. Oxygen sensing by metazoans: the central role of the HIF hydroxylase pathway. *Mol. Cell* **30**, 393–402 (2008).
32. Epstein, A. C. *et al.* *C. elegans* EGL-9 and mammalian homologs define a family of dioxygenases that regulate HIF by prolyl hydroxylation. *Cell* **107**, 43–54 (2001).
33. Saucedo, L. J. & Edgar, B. A. Filling out the Hippo pathway. *Nat. Rev. Mol. Cell Biol.* **8**, 613–621 (2007).
34. Badouel, C., Garg, A. & McNeill, H. Herding Hippos: regulating growth in flies and man. *Curr. Opin. Cell Biol.* **21**, 837–843 (2009).
35. Halder, G. & Johnson, R. L. Hippo signaling: growth control and beyond. *Development* **138**, 9–22 (2011).
36. Irvine, K. D. Integration of intercellular signaling through the Hippo pathway. *Semin. Cell Dev. Biol.* **23**, 812–817 (2012).
37. Pouyssegur, J., Dayan, F. & Mazure, N. M. Hypoxia signalling in cancer and approaches to enforce tumour regression. *Nature* **441**, 437–443 (2006).

METHODS

Cell culture and transfection. HEK293T, HeLa and MDA-MB-231 cell lines were from the American Type Culture Collection and were cultured under conditions specified by the manufacturer. Hypoxic conditions were achieved with a hypoxia chamber (Billups-Rothenberg) flushed with a gas mixture of 1% O₂, 5% CO₂ and 94% N₂. Plasmids were transfected into cells with Lipo2000 according to the manufacturer's instruction.

Expression constructs. The mammalian expression plasmids for human HIF1 α , SIAH1, SIAH2 and YAP were generated by PCR and cloned in pFLAG-CMV-4 or pcDNA4-TO-Myc-His-B expression vectors. The mammalian expression plasmids for Myc-LATS1 and Myc-LATS2 were generated by insertion of LATS1 or LATS2 cDNA in-frame into the pcDNA3.0 vector. Recombinant GST fusion proteins GST-SIAH2 and 6 \times His-LATS2 (403–720) were cloned in pGEX-4T-1 vector and pET28a vector respectively. All SIAH2, LATS2 and YAP mutants were made using the Quick-Change Site Mutagenesis Kit (TransGen Biotech). All of the constructs generated were confirmed by DNA sequencing. HRE-luciferase reporter vector was a gift from Y. Luo (Tsinghua University, China). HA-VHL expression vector was a gift from Y. Chen (Tsinghua University, China).

Immunoblotting. Cells were lysed in lysis buffer (150 mM NaCl, 20 mM Tris, pH 7.4, 1 mM EGTA, 1 mM EDTA, 1% NP-40, 2.5 mM sodium pyrophosphate, 1 mM Na₂VO₄, 10% glycerol and protease inhibitors). Equivalent protein quantities were subjected to SDS-PAGE, and transferred to nitrocellulose membranes. Membranes were blocked with 5% non-fat milk or 5% BSA for 1 h at room temperature and then probed with the indicated primary antibodies, followed by the appropriate HRP-conjugated anti-mouse/rabbit (KPL) or anti-goat (Beijing CoWin Biotech) secondary antibodies. Immunoreactive bands were visualized with chemiluminescence kits (Engreen Biosystem). The following antibodies were used: antibodies against SIAH2 (1:500, Sigma, S7945, clone SIAH2-369), actin (1:10,000, Sigma, A5441, clone AC-15), Flag (1:1,000, Sigma, F1804, clone M2), CYR61 (1:500, Santa Cruz, sc-13100), CTGF (1:500, Santa Cruz, sc-14939), MYC (1:1,000, Santa Cruz, sc-40, clone 9E10), HA (1:1,000, Abmart, M20003, clone 26D11), His (1:1,000, Santa Cruz, sc-8036, clone H-3), LATS2 (1:1,000, Abcam, ab70565), p-S127-YAP (1:1,000, Cell Signaling, 4911), OH-Pro564-HIF1 α (1:1,000, Cell Signaling, 3434, clone D43B5), YAP (1:1,000, Epitomics, 2060-1, clone EP1674Y), HIF1 α (1:1,000, Epitomics, 2015-1, clone EP1215Y) and ubiquitin (1:1,000, Enzo Life Sciences, PW8805, clone FK1). The ImageJ program (<http://rsbweb.nih.gov/ij/download.html>) was used for densitometric analyses of western blots, and the quantification results were normalized to the loading control.

Immunoprecipitation. Cells were collected and lysed in 0.5 ml lysis buffer plus protease inhibitors (Roche) for 50 min on a rotor at 4 °C. After 12,000g centrifugation for 15 min, the lysates were immunoprecipitated with 2 μ g specific antibody overnight at 4 °C, and 30 μ l A/G agarose beads (Santa Cruz, SC-2003) were washed and then added for an additional 3 h. Thereafter, the precipitants were washed five times with lysis buffer, and the immune complexes were boiled with loading buffer for 5 min and analysed by SDS-PAGE. The following antibodies were used for immunoprecipitation: antibodies against MYC (Santa Cruz, sc-40, clone 9E10), Flag (Sigma, F1804, clone M2), HA (Abmart, M20003, clone 26D11), LATS2 (Abcam, ab70565) and YAP (Epitomics, 2060-1, clone EP1674Y).

Immunoprecipitation and mass spectrometric analysis of SIAH2-associated proteins. Ten 10-cm dishes of HEK293T cells were transiently transfected with Flag-SIAH2^{RM}. Twenty-four hours later, cells were collected and lysed in lysis buffer followed by immunoprecipitation with anti-Flag antibody overnight at 4 °C. The precipitants were extensively washed with lysis buffer then boiled with SDS loading buffer and subjected to SDS-PAGE. Gels with total proteins were excised, followed by in-gel digestion and analysis by LC-MS/MS.

Chromatin immunoprecipitation assay. Cells were cultured under normoxic or hypoxic conditions for 6 h. Thereafter, cells were treated with 1% formaldehyde for 10 min at room temperature and then quenched by glycine addition. Cells were collected by scraping and cell nuclei were extracted by the Nuclear Extract Kit (Sangon Biotech, BSP009). Sonicated nuclear lysates were pre-cleared with protein A/G agarose beads and immunoprecipitated with 2 μ g anti-HIF1 α (Abnova, MAB1892, clone H1alpha67), anti-YAP (Epitomics, 2060-1, clone EP1674Y) antibody or nonspecific IgG antibody. Agarose beads were extensively washed, eluted with a buffer consisting of 1% SDS. DNA-protein complex were decrosslinked by addition of proteinase K and then incubated at 65 °C overnight. DNA was obtained by the DNA Extraction Kit (Axygen). The primer for the -1216 to -883 region of the human VEGF promoter containing the HRE site is 5'-CACAGACCTTCACAGCCATC-3' and 5'-CCCAGCGTAGACAGTTGAGT-3'.

Immunofluorescence microscopy. Cells were seeded on coverslips. Cells were fixed with 4% paraformaldehyde (Dingguo changsheng Biotechnology) for 10 min at room temperature, and then permeabilized with 0.1% Triton X-100 with DAPI on ice. After blocking in goat serum for 1 h, slides were incubated with primary antibody for 1 h at room temperature or at 4 °C overnight, washed 3 times with PBS, and then incubated with FITC- or CY3-conjugated secondary antibodies (Invitrogen, 1:1,000) for 1 h at room temperature. The following antibodies were used for immunofluorescence: antibodies against YAP (1:100, Epitomics, 2060-1, clone EP1674Y), HIF1 α (1:100, GeneTex, GTX628480, clone GT10211) and Ki67 (1:1,000, Abcam, ab15580). The slides were then washed 3 times with PBS and mounted. Cell images were captured with a confocal microscope (Leica).

HRE-luciferase reporter gene assay. Cells were transiently transfected with the HRE-firefly-luciferase construct in combination with a *Renilla* luciferase plasmid. After 24 h, cells were incubated at normoxia or hypoxic conditions for 6 h, and then collected and the luciferase activity was measured using the Dual Luciferase Reporter Assay System Kit (Promega) according to the manufacturer's protocol. Activity was assayed in three independent experiments and is shown as the average mean \pm standard deviation (s.d.).

GST pulldown. Recombinant GST-SIAH2, GST-SIAH2^{RM} and 6 \times His-LATS2 (403–720) proteins were produced in *Escherichia coli* BL21 cells and purified with glutathione-Sepharose 4B (GE Healthcare) or Ni-NTA resin (GE Healthcare) respectively according to standard protocols. Ten micrograms of GST or GST fusion proteins was incubated at 4 °C overnight with 10 μ g purified 6 \times His-LATS2 (403–720) and 20 μ l of glutathione-Sepharose beads. Supernatants were collected as input and the Sepharose beads were then extensively washed 5 times with lysis buffer and resuspended in SDS loading buffer and boiled. A quarter of the sample buffer was loaded in 12% SDS-PAGE for detection with anti-His antibody.

In vivo ubiquitylation assay. Cells were transiently transfected with plasmids expressing HA-ubiquitin and Myc-LATS2 alone or together with Flag-SIAH2^{RM}. Twenty four hours after transfection, cells were treated with 10 μ M MG132 (Selleckchem S2619) for 6 h before collection. Cells were washed with cold PBS and then lysed in 200 μ l of denaturing buffer (150 mM Tris-HCl pH 7.4, 1% SDS) by sonication and boiling for 10 min. Lysates were added with lysis buffer to 1 ml and immunoprecipitated using 2 μ g anti-c-Myc antibody and subjected to western blotting with anti-HA or anti-Myc antibody to detect ubiquitylation. For LATS2 endogenous ubiquitylation assay, Scramble or SIAH2-knockdown cells were treated with 10 μ M MG132 for 6 h before collection. Lysates were immunoprecipitated using 2 μ g anti-LATS2 antibody and subjected to ubiquitylation analysis by western blotting with anti-LATS2 or anti-ubiquitin antibody.

In vitro ubiquitylation assay. *In vitro* ubiquitylation assays were carried out in ubiquitylation buffer (50 mM Tris, pH 7.4, 5 mM MgCl₂, 2 mM dithiothreitol) with human recombinant E1 (100 ng, Abcam), human recombinant E2 UbcH5c (200 ng, Upstate), His-tagged ubiquitin (10 μ g, Upstate). LATS2 or LATS2 lysine mutants were immunopurified from cells lysates of cells transfected with Myc-LATS2 or its mutants. GST-SIAH2 or GST-SIAH2^{RM} as an E3 ligase was expressed and purified from *Escherichia coli* BL21 cells. Two micrograms of GST or GST-SIAH2 or GST-SIAH2^{RM} proteins was used in corresponding ubiquitylation reactions. Reactions (30 μ l volume) were incubated at 30 °C for 2 h and subjected to ubiquitylation analysis by western blotting using anti-Myc antibody.

Cycloheximide chase assay. The half-life of endogenous or ectopically expressing LATS2 was determined by cycloheximide (CHX) chase assay. Scramble or SIAH2-knockdown cells were individually seeded in 60 mm dishes, or cells were transfected with 1 μ g of Flag-vector, Flag-SIAH2 or Flag-SIAH2^{RM} with or without 1.5 μ g Myc-LATS2. Twenty-four hours later, cells were treated with CHX (100 μ g ml⁻¹) and collected at the indicated time points for sonication in the denaturing buffer (150 mM Tris-HCl pH 7.4, 1% SDS), then the equal amount of boiled lysates were analysed by western blotting.

Lentiviral shRNA cloning, production and infection. To generate YAP-, SIAH2-, and SIAH2- and LATS2-knockdown cells, oligonucleotides were cloned into pLKO.1 with the AgeI and EcoRI sites. Lentiviral packaging plasmids psPAX2 and pMD2.G were co-transfected with the backbone plasmid into HEK293T cells for virus production. Cells were selected in 2.5 μ g ml⁻¹ puromycin in culture medium. The oligonucleotide pairs used were as follows: YAP no. 1 (5'-CCGGCCCAAGTTAATGTTCAACAATCTCGAGATTGGTGAACATTTAACTGGGTTTTG-3' and 5'-AATTCAAAAACCCAGTAAATGTTCCAAATCTCGAGATTGGTGAACATTTAACTGGG-3'); YAP no. 2 (5'-CCGGCCCAAGCTAGATAAAGAAGCTCGA GTTCTTTATCTAGCTTGGTGGCTTTTGG-3' and 5'-AATTCAAAAAGCCACC AAGCTAGATAAAGAAGCTCGAGTTCTTTATCTAGCTTGGTGGC-3'); SIAH2

no. 1 (5'-CCGGGCTACAGACTGGAGTTGAATCTCGAGATTCAACTCCAGTCTGTAGGCTTTTTG-3' and 5'-AATTCAAAAAGCCTACAGACTGGAGTTGAACTCTCGAGATTCAACTCCAGTCTGTAGGC-3'); SIAH2 no. 2 (5'-CCGGGCTGGCTAATAGACACTGAATCTCGAGATTCAACTCCAGTCTGTAGGCTTTTTG-3' and 5'-AATTCAAAAAGCTGGCTAATAGACACTGAATCTCGAGATTCAACTCCAGTCTGTAGGCTTTTTG-3'); LATS2: (5'-CCGGGCTGGCTAATAGACACTGAATCTCGAGATTCAACTCCAGTCTGTAGGCTTTTTG-3' and 5'-AATTCAAAAAGCA GATTGTGCGGGTCATTAACCTCGAGTTAATGACCCGCACAATCTGC-3').

RNA isolation and real-time PCR. Total RNA was isolated from cultured cells using Trizol reagent (Roche). cDNA was synthesized by reverse transcription using oligo (dT) and subjected to real-time PCR with *CTGF*, *CYR61*, *VEGF*, *HIF1 α* , *LATS2*, *SIAH2*, *ACTB* primers in the presence of Cyber green PCR-Mix (Roche). Relative abundance of mRNA was calculated by normalization to *ACTB* mRNA. The following primer pairs were used to detect the mRNA levels of the following genes by RT-qPCR: *CYR61* (5'-GGTCAAAGTTACCGGGCAGT-3' and 5'-GGAGGCATCGAATCCAGC); *CTGF* (5'-ACCGACTGGAAGACACGTTTG-3' and 5'-CCAGGTCCAGCTTCGCAAGG-3'); *VEGF* (5'-GGCTGGCAACATAACAGAGAA-3' and 5'-CCCCACATCTATACACCTCC-3'); *SIAH2* (5'-CGCCAGAAGTTGAGCTGCT-3' and 5'-TGGTGGCATACTACAGGGAA-3'); *LATS2* (5'-ACCCAAAGTCCGACCTTAT-3' and 5'-CATTTCGGGTTCACTTCTGC-3'); *HIF1 α* (5'-CACACAGGACAGTACAGGAT-3' and 5'-CGTGTGAATAATACCACTCACA-3'); *ACTB*: (5'-CATGTACGTTGCTATCCAGGC-3' and 5'-CTCCTTAATGTCACGCA CGAT-3'). Data were analysed from three independent experiments and are shown as the average mean \pm s.d.

Cell proliferation and viability assay. MDA-MB-231 cells (2×10^5) stably expressing Flag-vector, Flag-SIAH2 or Flag-SIAH2^{RM} were seeded on 6-well plates in 2 ml DMEM supplemented with 10% FBS. Cell proliferation rate was measured through counting cell numbers at indicated time points. Cell viability was measured using a colorimetric MTT assay. Three thousand MDA-MB-231 cells stably expressing Flag-vector, Flag-SIAH2 or Flag-SIAH2^{RM} were seeded on 96-well plates. Thirty-six hours later, cells were treated with MTT (0.5 mg ml⁻¹) for 5 h. The samples were dissolved in dimethylsulphoxide and MTT absorbance was read at 570 nm.

Colony-formation assay. MDA-MB-231 cells (100) harbouring scramble shRNA, SIAH2 shRNA or SIAH2 and LATS2 shRNAs were seeded on 60 mm plates in 5 ml DMEM supplemented with 10% FBS. Twenty-four hours later, cells were moved into a hypoxia chamber (1% O₂) and cultured under hypoxic conditions for 3 weeks until foci were evident. Cells were fixed with 4% paraformaldehyde, and then colonies were stained with 1% crystal violet and counted.

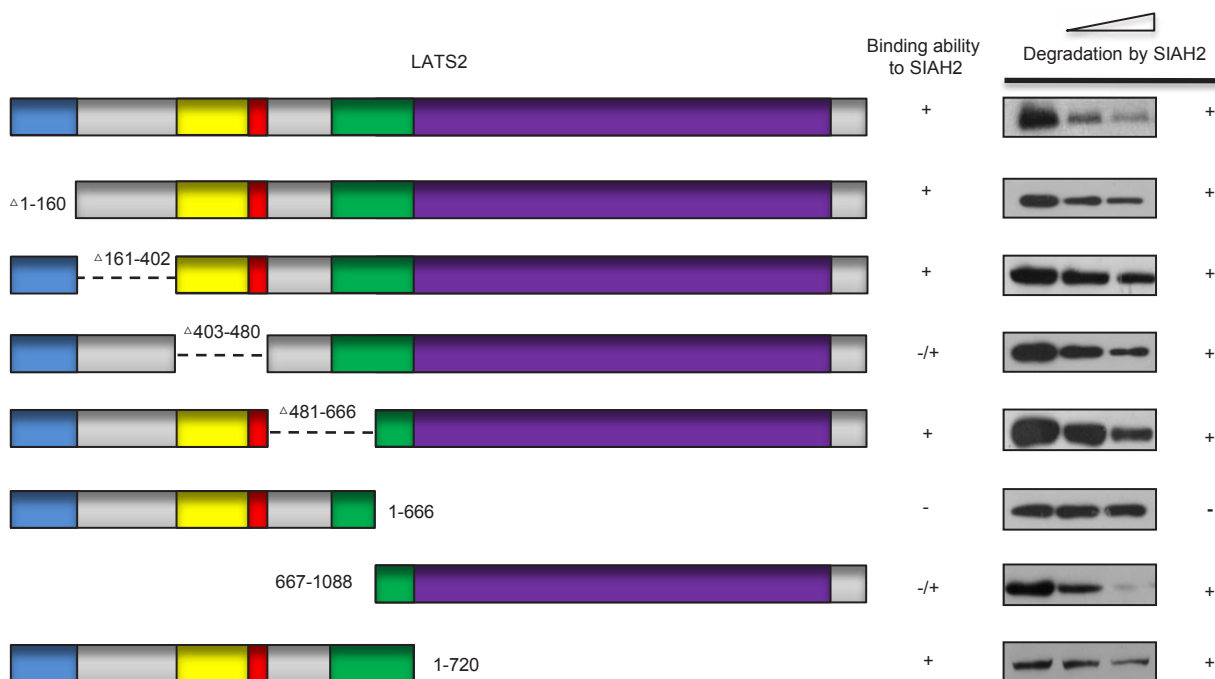
Flow cytometry analysis. Cells were cultured under hypoxic conditions for 24 h. After washing with cold PBS, cells were digested with trypsin, collected and resuspended and double stained with Annexin V-FITC and propidium iodide. Ten thousand cells were analysed by flow cytometry for apoptotic cells.

Data were analysed from three independent experiments and are shown as the average mean \pm s.d.

In vivo tumorigenesis study. All mouse experiments were approved by the Institutional Animal Care and Use Committee at the College of Life Sciences at Nankai University. MDA-MB-231 breast cancer cells (2×10^6 in 100 μ l PBS) were injected subcutaneously into the armpit of six- to eight-week-old female nude mice. Tumour size was measured every four days one week after the implantation and tumour volume was analysed by using the formula $V = 0.5 \times L \times W^2$ (V : volume, L : length, W : width). A month later, the subcutaneous tumours were surgically removed, weighed and photographed. No statistical method was used to predetermine sample size for each group. The experiments were not randomized.

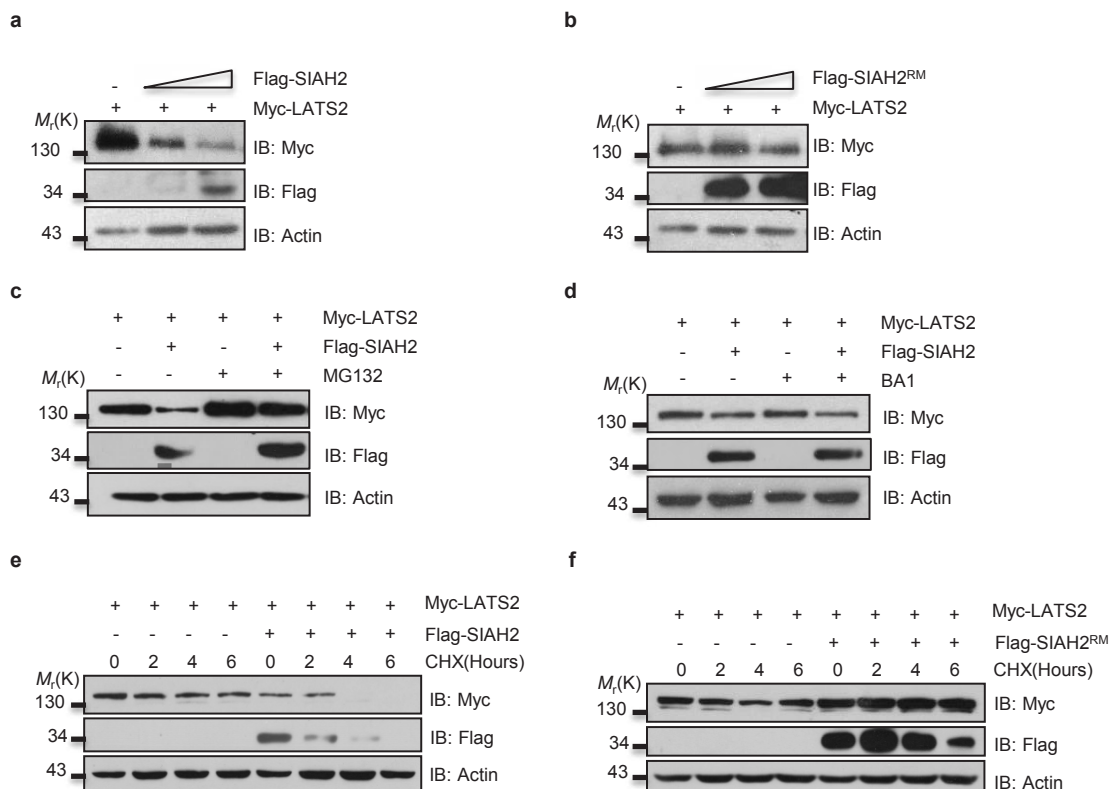
Patient study and immunohistochemistry. The breast cancer tissue microarrays were purchased from US Biomax. These tissue microarrays consist of 203–204 analysable cases of invasive breast carcinoma and 70–77 analysable cases of normal breast tissue. For antigen retrieval, the slides were rehydrated and then treated with 10 mM sodium citrate buffer (pH 6.0) heated for 20 min at 95 °C. The samples were pretreated with 5% goat serum for 1 h to block antibody nonspecific binding and then incubated with the indicated antibodies at 4 °C overnight. The samples were treated with 0.3% H₂O₂ for 30 min to block endogenous peroxidase activity and then incubated with HRP-conjugated secondary antibody for 1 h at room temperature. The following antibodies were used for immunohistochemistry: antibodies against LATS2 (1:200, Abcam, ab70565), SIAH2 (1:40, Novus biologicals, NB110-88113, clone 24E6H3), HIF1 α (1:100, Epitomics, 2015-1, clone EP1215Y), p-S127-YAP (1:100, Cell Signalling, 4911), YAP (1:100, Epitomics, 2060-1, clone EP1674Y), Ki67 (1:1,000, Abcam, ab15580) and Endomucin (1:100, eBioscience, 14-4321). Immunoreactive signal was visualized with a DAB Substrate Kit (MaidXin Bio). Protein expression levels of all the samples were scored as four grades (0–3) according to the percentage of immunopositive cells and immunostaining intensity. Grade 0–3 represent: 0 (no expression), 1 (low expression), 2 (moderate expression), 3 (high expression). Grade 0 and 1 were defined as low expression and Grade 2 and 3 were defined as high expression. The χ^2 test was used for analysis of the significance of SIAH2 or LATS2 with tumour or normal tissue and the correlation between LATS2 and SIAH2.

Statistics and repeatability of experiments. All error bars indicate s.d. Statistical comparisons of means were made using the unpaired Student's two-tailed t -test for two data sets using Excel (Microsoft). The data analysed by the t -test meet normal distribution. For correlation between LATS2 and SIAH2 protein levels in human breast tumours, statistical significance was determined by χ^2 test. The R value was the correlation coefficient. For statistical tests, $P < 0.05$ was used as the criterion for statistical significance. The variance was similar between groups that were being statistically compared and no samples were excluded from the analysis. The experiments were repeated at least three times. The investigators were not blinded to allocation during experiments and outcome assessment.



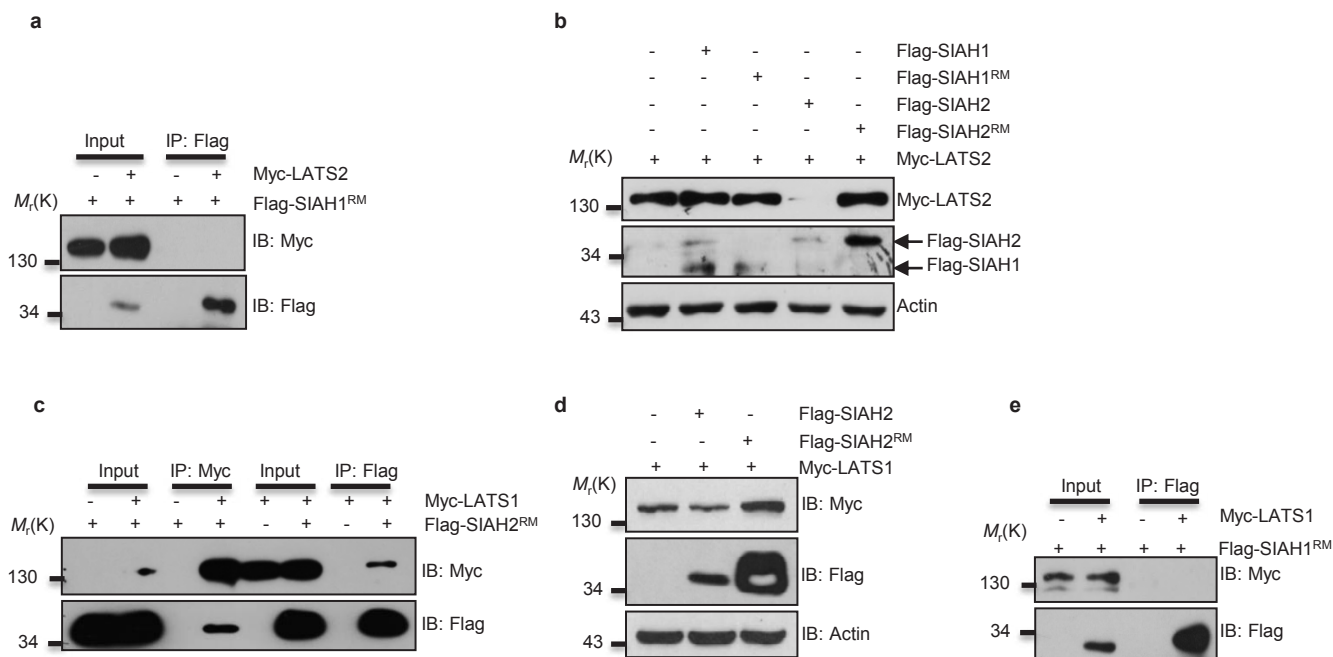
Supplementary Figure 1 Schematic drawing of LATS2 deletion mutants and their responses to interaction with and degradation by SIAH2. A schematic diagram of LATS2 deletion mutants is shown on the left panel. Blue represents as LATS Conserved Domain 1(LCD1) (aa.1-160), yellow as LATS Conserved Domain 2(LCD2) (aa.403-463), red as PAPA repeat (aa.467-480), green as Protein Binding Domain (PBD) (aa.618-720), purple as Kinase Domain. LATS2

binding activity to SIAH2 is shown in the middle panel as assayed in Fig 1d. "+" indicates as binding, "-" as no binding, and "-/+" as less binding. The right panel shows the responses of LATS2 mutants to SIAH2-induced degradation. Cells expressing constant amounts of Myc-LATS2 mutant and increasing amounts of Flag-SIAH2 were subjected to immunoblotting. "+" indicates response to SIAH2-induced degradation and "-" indicates non-response.



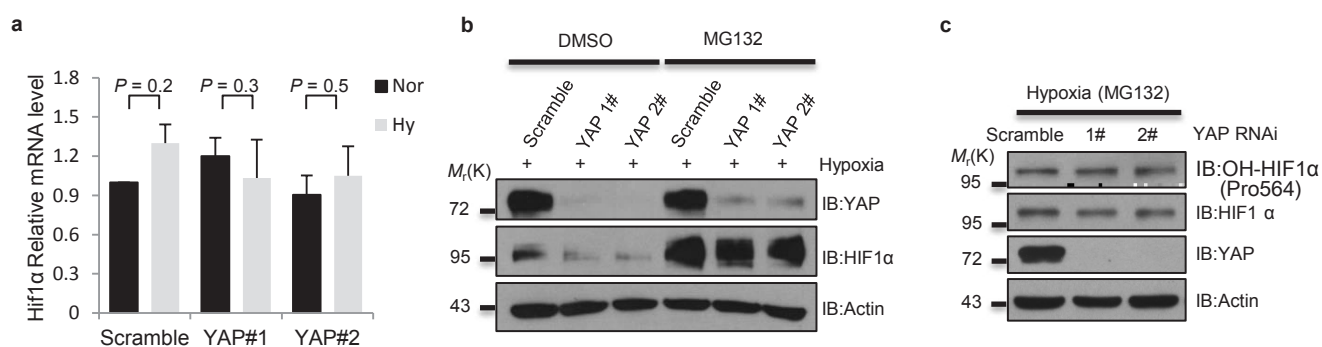
Supplementary Figure 2 SIAH2 destabilizes LATS2 through proteasome. **(a, b)** LATS2 degradation was dosage-dependent on SIAH2 **(a)**, but not on SIAH2^{RM}, an E3 ligase-activity-dead mutant of SIAH2 **(b)**. **(c, d)** SIAH2-mediated LATS2

degradation was inhibited by proteasomal inhibitor MG132 **(c)**, but not by lysosomal inhibitor BA-1 **(d)**. **(e, f)** The half-life of LATS2 was shortened by SIAH2 **(e)** but not by SIAH2^{RM} **(f)** in cycloheximide chase assays.



Supplementary Figure 3 LATS1/2 is specifically regulated by SIAH2 but not by SIAH1. **(a)** No co-immunoprecipitation of exogenously expressed Myc-LATS2 by Flag-SIAH1^{RM}. **(b)** LATS2 degradation is specifically promoted by SIAH2 but not by SIAH1. **(c)** Co-immunoprecipitation of

exogenous expressed Flag-SIAH2 by Myc-LATS1 and vice versa. **(d)** LATS1 stability is regulated by SIAH2 but not by SIAH2^{RM}. **(e)** No co-immunoprecipitation of exogenously expressed Myc-LATS1 by Flag-SIAH1^{RM}.



Supplement Figure 4 YAP protects HIF1 α from proteasomal degradation under hypoxia. **(a)** Scramble and YAP knockdown MDA-MB-231 cells were cultured under hypoxic conditions. Total RNA was extracted and subjected to RT-qPCR analysis for HIF1 α mRNA expression. **(b)** MG132 stabilized HIF1 α in YAP knockdown cells under hypoxic conditions. **(c)** Scramble

and YAP knockdown MDA-MB-231 cells were cultured under hypoxic conditions in the presence of MG132. Protein expressions were analyzed by immunoblotting with indicated antibodies. Data in **a** is the mean of n=3 independent experiments and error bars indicate s.d.. Two-tailed, unpaired Student's t-test.

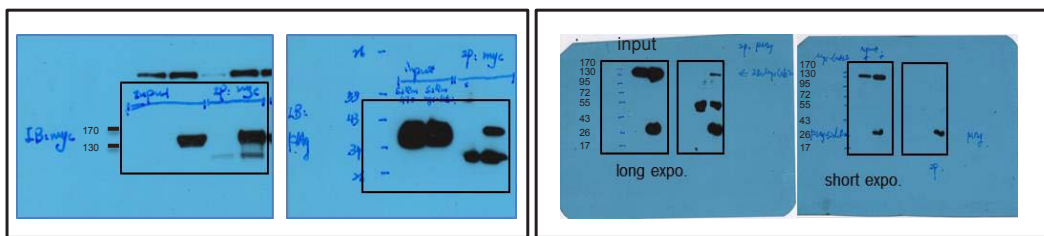


Figure 1a

Figure 1b

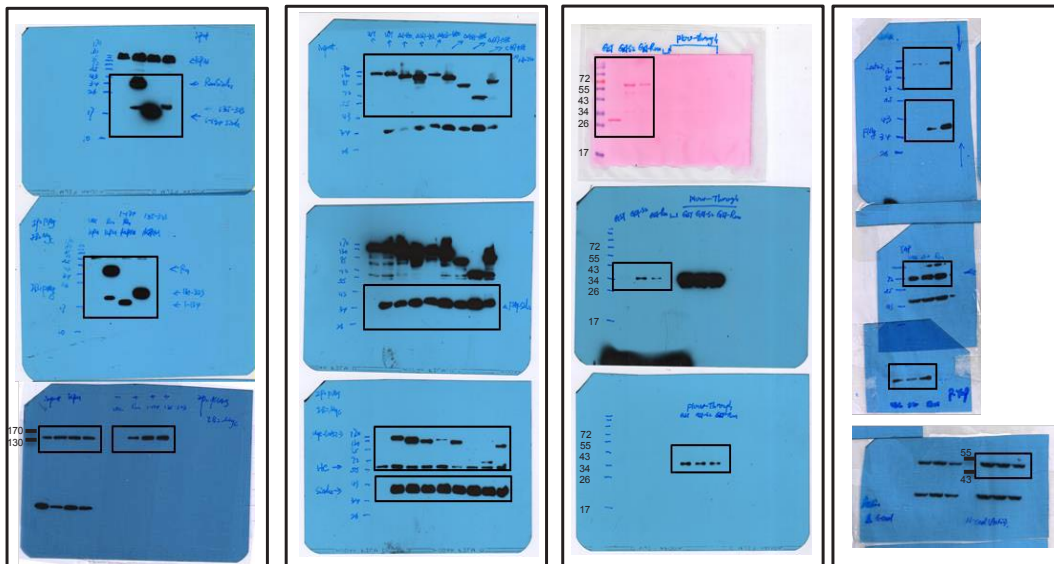


Figure 1c

Figure 1d

Figure 1f

Figure 2a

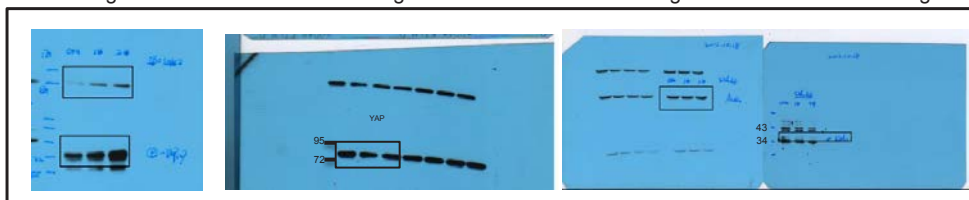


Figure 2b



Figure 2c

Figure 2e

Figure 2g

Supplement Figure 5 continued Uncropped images of key blots/gels.

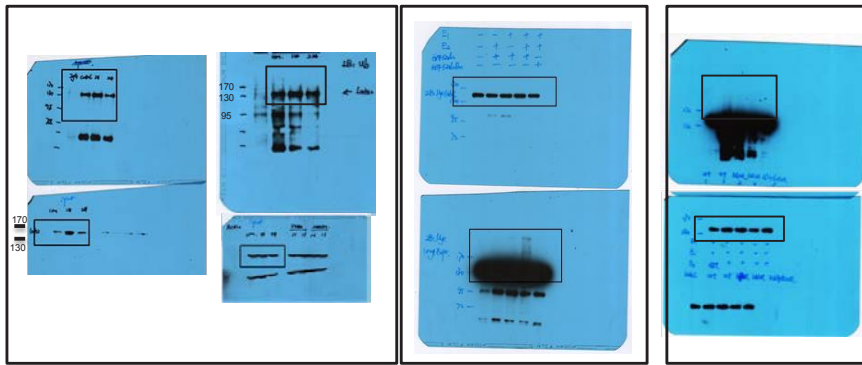


Figure 2h

Figure 2i

Figure 2l

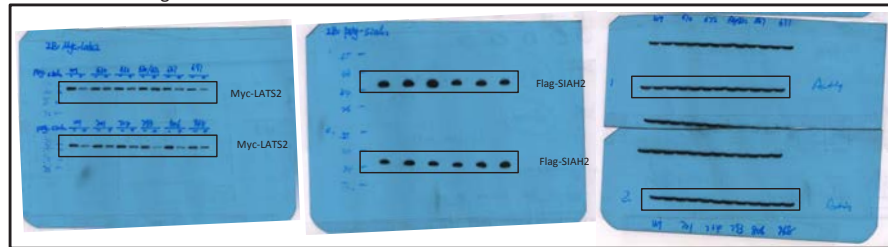


Figure 2k

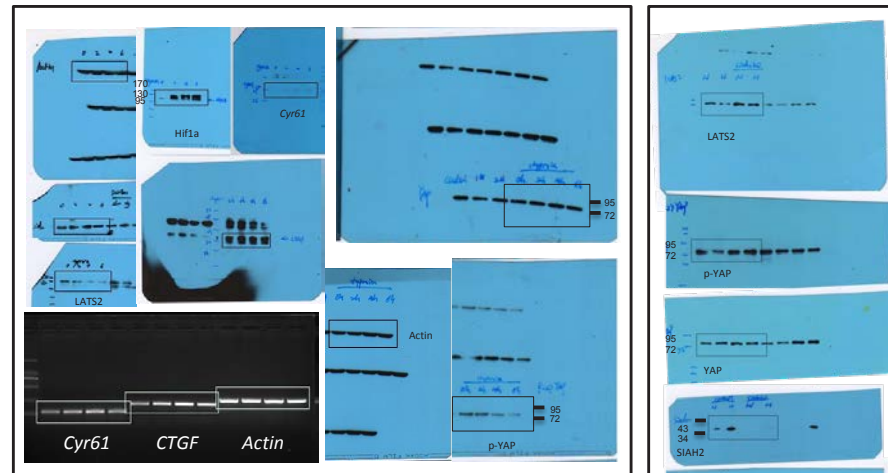


Figure 3a



Figure 3g

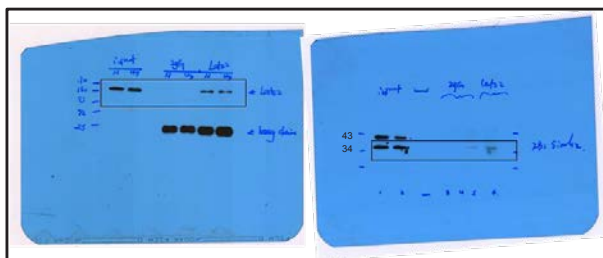


Figure 3e

Supplement Figure 5 continued Uncropped images of key blots/gels.

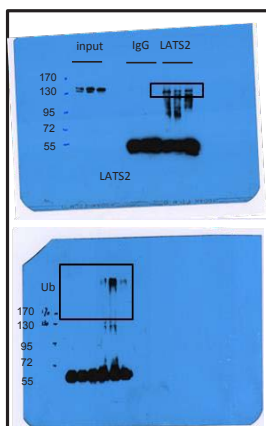


Figure 3i

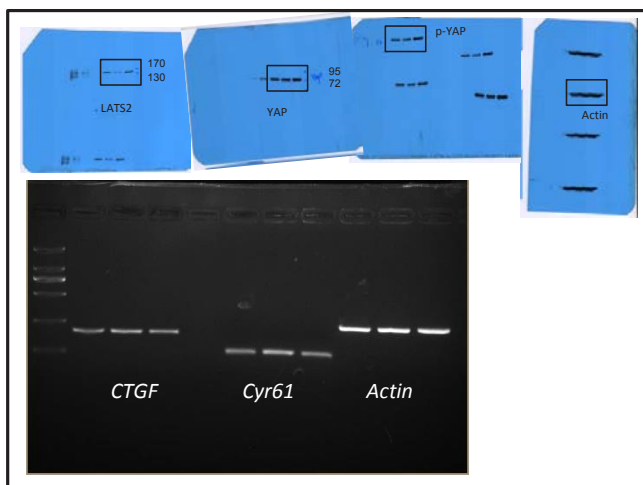


Figure 3j

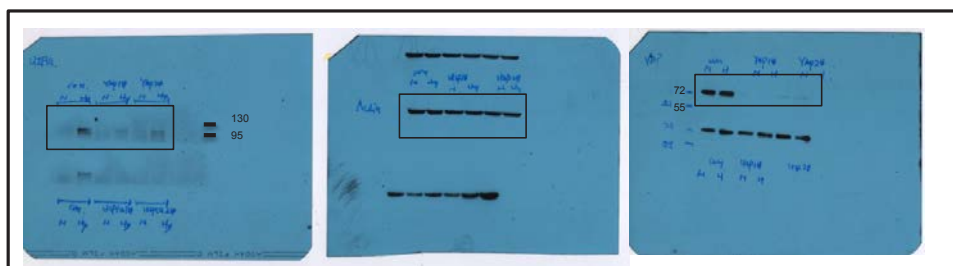


Figure 5a

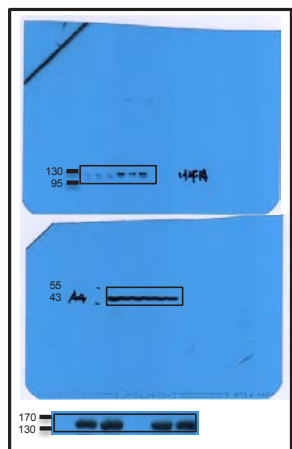


Figure 5i

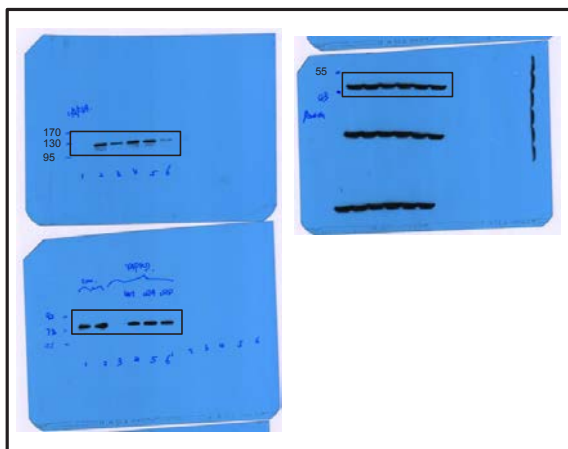


Figure 5j

Supplement Figure 5 continued Uncropped images of key blots/gels.

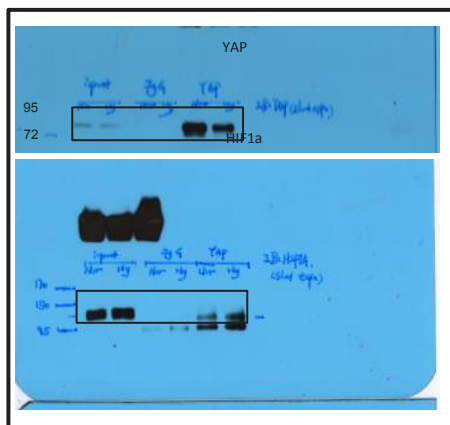


Figure 5m

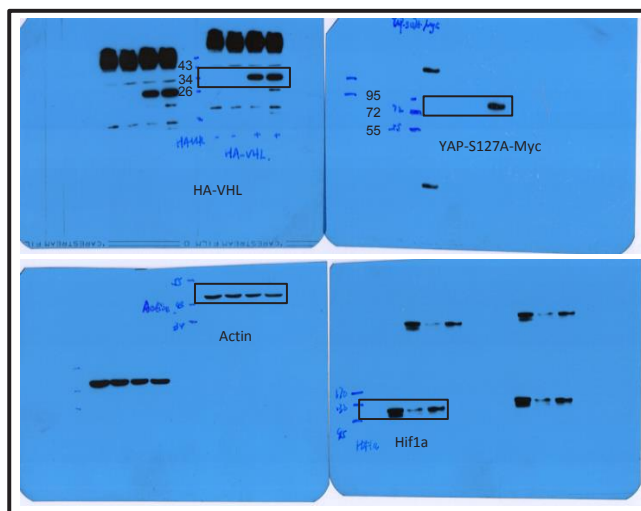


Figure 5o

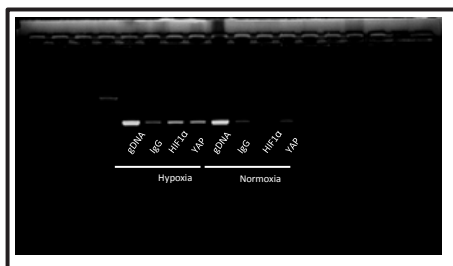


Figure 5n

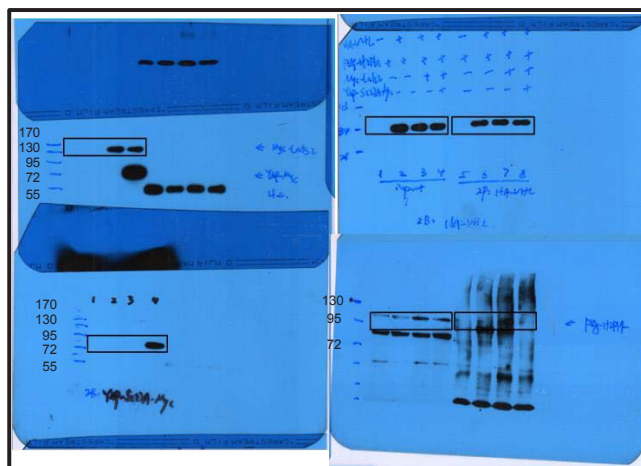


Figure 5p

Supplement Figure 5 continued Uncropped images of key blots/gels.

Supplementary Table 1: Identification of LATS2 as a SIAH2-associated protein.

Protein	Number of peptides
2-oxoglutarate dehydrogenase	35
2-oxoglutarate dehydrogenase-like	16
Serine/threonine-protein kinase LATS2	5
Homeodomain-interacting protein kinase	4
SH3 domain-containing RING finger protein 3 (POSH2)	4
E3 ubiquitin-protein ligase SH3RF1 (POSH)	1

Supplementary Table 1 Identification of LATS2 as a SIAH2-associated protein. LATS2 and known interacting partners of SIAH2 and their related proteins are listed together with the number of peptides for each protein identified by mass spectrometry.

Supplementary Table 2: Species aligned for conservation of LATS2 lysine residues.

No.	Species
1	<i>Homo sapiens</i>
2	<i>Mus musculus</i>
3	<i>Rattus norvegicus</i>
4	<i>Monodelphis domestica</i>
5	<i>Pan troglodytes</i>
6	<i>Pongo abelii</i>
7	<i>Nomascus leucogenys</i>
8	<i>Ailuropoda melanoleuca</i>
9	<i>Sus scrofa</i>
10	<i>Bos taurus</i>
11	<i>Ovis aries</i>
12	<i>Equus caballus</i>
13	<i>Loxodonta africana</i>
14	<i>Canis familiaris</i>
15	<i>Felis catus</i>
16	<i>Myotis lucifugus</i>
17	<i>Sarcophilus harrisii</i>
18	Tasmanian devil
19	<i>Callithrix jacchus</i>
20	<i>Oryctolagus cuniculus</i>
21	<i>Gallus gallus</i>
22	<i>Meleagris gallopavo</i>
23	<i>Anas platyrhynchos</i>
24	<i>Ficedula albicollis</i>
25	<i>Taeniopygia guttata</i>
26	<i>Xenopus tropicalis</i>
27	<i>Pelodiscus sinensis</i>
28	<i>Danio rerio</i>
29	<i>Drosophila melanogaster</i>

Supplementary Table 2 Species aligned for conservation of LATS2 lysine residues. Human LATS2 were aligned with the listed 28 species to identify those conserved lysine residues in Human LATS2 (667-1088).

Supplementary Table 3: LATS2 protein is downregulated and inversely correlated with SIAH2 protein levels in human breast cancer

	LATS2-low	LATS2-high	Total
Breast tumor	138 (68.0%)	65 (32.0%)	203
Normal tissue	18 (25.7%)	52 (74.3%)	70
$P = 7.2 \times 10^{-10}$			$R = -0.37$

	SIAH2-low	SIAH2-high	Total
Breast tumor	105 (51.5%)	99 (48.5%)	204
Normal tissue	69 (89.6%)	8 (10.4%)	77
$P = 4.3 \times 10^{-9}$			$R = 0.35$

	LATS2-low	LATS2-high	Total
SIAH2-low	60 (57.7%)	44 (42.2%)	104
SIAH2-high	78 (78.8%)	21 (21.2%)	99
Total	138	65	203
$P = 1.3 \times 10^{-3}$			$R = -0.23$

Supplementary Table 3 LATS2 protein is downregulated and inversely correlated with SIAH2 protein levels in human breast cancer. LATS2 and SIAH2 protein expression status in normal breast and breast carcinoma specimens. Correlation between LATS2 and SIAH2 protein levels in human breast tumors. Statistical significance was determined by χ^2 test. R is the correlation coefficient.

Supplementary Table 4: Statistics source data

Fig. 4a	0h			48h			
	Vector	SIAH2	SIAH2 ^{RM}	Vector	SIAH2	SIAH2 ^{RM}	Vector
#1	2.00	2.00	2.00	4.85	7.50	4.80	10.30
#2	2.00	2.00	2.00	6.50	7.00	4.30	10.80
#3	2.00	2.00	2.00	4.75	6.65	4.20	12.25
Mean	2.00	2.00	2.00	5.37	7.05	4.43	11.12
S.D.	0.00	0.00	0.00	0.98	0.43	0.32	1.01

Fig. 4b	Vector	SIAH2	SIAH2 ^{RM}
#1	0.20	0.48	0.27
#2	0.32	0.49	0.23
#3	0.22	0.60	0.24
#4	0.25	0.49	0.21
Mean	0.25	0.51	0.24
S.D.	0.05	0.05	0.02

Fig. 4c	Scramble	SIAH2 RNAi	SIAH2&LATS2 RNAi
#1	75.00	35.00	57.00
#2	86.00	33.00	65.00
#3	90.00	36.00	70.00
Mean	83.67	34.67	64.00
S.D.	7.78	1.41	5.66

Fig. 4d	Scramble	SIAH2 RNAi	SIAH2&LATS2 RNAi
#1	23.08	41.96	24.76
#2	22.01	36.43	23.06
#3	22.66	38.89	23.21
Mean	22.58	39.09	23.68
S.D.	0.44	2.26	0.77

Supplementary Table 4 Statistics source data. Statistics source data of Figure 4a-d